MCIT
Modeling, control & information technologies

# Collection and processing of bearing vibration data for their technical condition classification by machine learning methods

https://doi.org/10.31713/MCIT.2021.02

Ruslan Babudzhan, Danylo Krasii, Oleksii Vodka, Ivan Zadorozhniy
Department of dynamic and strength of machines
NTU "KhPI"
Kharkiv, Ukraine

Kostiantyn Isaienkov, Ruben Melkonian, Michael Yushchuk
Quantum inc
Lewes, Delaver, USA

***Abstract* — An experimental research facility has been developed to receive vibration signals from mechanisms with installed rolling bearings. A control block for all equipment has been created. For the repeatability of the experiment, an external microcontroller with a programmed proportional-integral-derivative regulator was used.**

**Experiments were carried out to obtain initial data for different types of bearings. The processed data were grouped and made publicly available for further research. It is proposed to solve the problem of emergency stop of the generator, arising during operation due to bearings worn, by recognizing the pre-emergency conditions of rotary rig based on the use of advanced machine learning techniques: to highlight the signs of vibration and build clusters according to the degree of worn)**

***Keywords* — vibration; signals; vibrodiagnostics; signal statistics; feature extraction; exploratory data analysis; machine learning; Fourier transform.**

## I. INTRODUCTION

Signal processing and analysis is widely used in radio electronics, seismic analysis, speech recognition, and vibration diagnostics of industrial structures. From the point of view of a variety of tasks and applications of signal processing, vibration diagnostics of structures is one of the greatest interests. The development of new methods for analyzing vibrations of constructions is actively carried out today. The tasks of analyzing bearing assemblies as one of the most frequent places of failure of rotating machines have become very popular. The empirical approaches to vibrodiagnostics that are widespread now give relatively high-quality results and are actively used in industry today.

However, the classical methods presented, for example, in [1, 2, 3], have a limited range of applications and a fairly large amount of preparatory work on the use of these methods in applied problems. There is a shortage of expert analysts who are able to analyze spectrograms of vibration diagnostics of turbine generators, wind turbines, workbenches, etc., recorded by vibration sensors in real time [4].

Thus, it is necessary to develop automated intelligent systems for online monitoring of vibration conditions with the function of predicting emergency situations. The implementation of this method will help to classify the vibration states of bearings based on the use of neural network processing of vibration measurement data [5, 6]. This approach provides new opportunities for diagnosing defects in real mechanical engineering structures [7].

To build brand new algorithms for the mathematical analysis of vibrations in bearings, it is necessary to be familiarized with the classical methods of analysis both from the side of the experiment statement and from the side of the signal processing methodology for further drawing conclusions about the state of the structural unit. So, in work [8] the frequency of mechanical vibrations of a motor with a squirrel-cage rotor and an identical motor which operates under the eccentricity of a dynamic rotor are analyzed. Radial vibrations are modeled based on experimental data in no-load and nominal load modes. The focus is on vibration frequency and frequency variation. The need for further study of vibration recognition methods is indicated.

The method for analyzing the operation of bearings proposed in [9] is distinguished by a more detailed description of the diagnostics of the spectra of defect states. Work [10] describes a new approach to identifying bearing defects, namely, spectral images of vibration signals. Spectrum images are simply obtained by fast Fourier transform [11]. Such images are processed using two-dimensional principal component analysis (2DPCA) to reduce the size of the feature space, and then the minimum distance method is applied to the results obtained to classify bearing faults [12]. The purpose of this work is to develop an experimental setup for recording the vibration characteristics of various bearings, to conduct experimental research at the stand, and to create a data set for further research

## II. SET UP THE EXPERIMENT

To achieve this goal, a test bench has been developed and configured to simulate the operation of the rotor system. Vibration sensors have been used to monitor the state of mechanisms in an automatic mode, to classify the quality of bearings operation with deep learning methods. The test bench is shown in Fig. 1. The test bench drawing is shown on Fig. 2.

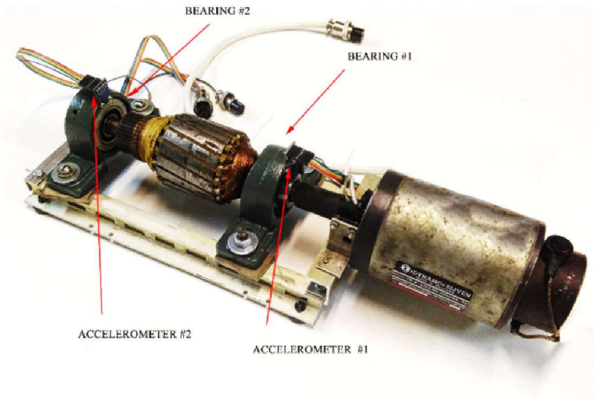


Figure 1. Mechanical part of the test bench

A Dynamo Sliven PIK 8 - 6 / 2.5 electric motor has been used in the design. The motor drives a shaft with an interruption ring mounted. Interrupts are sent to the analog-to-digital converter. The speed of rotation is calculated during operation for a closed-loop speed control system and is also recorded for subsequent processing. Accelerometers model GY-61 have been mounted on two bearing supports. A balanced weight of 3.5 kg has been attached between the struts. The bearing struts have been designed for bearings of the 6204 type, but with the help of nozzles, model 6202 has been used in the experiments.

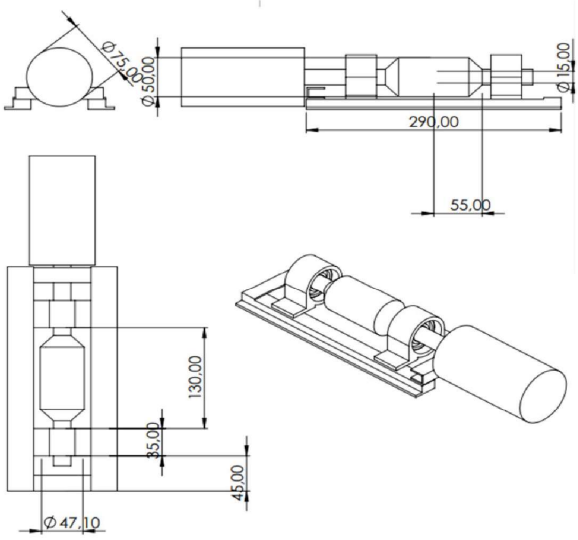


Figure 2. Test bench drawings

The control unit is powered by a standard current of 220 V. Inside the control unit there is a 30 V power supply powering a motor.

There are 2 control modes: manual and from an external microcontroller. DC Speed Controller HHORC-20A is used for external manual control.

External control comes from the Arduino. At the input, the Arduino receives the rotation speed, and at the output it supplies a PWM signal, the frequency of which is generated by the PID controller. The regulator has been tuned and calibrated so that the motor accelerates to 1500 rpm, then maintains this speed and then also slowly decelerates to 200 rpm. This has been done so that the experimental procedure is similar to each other for any bearing. Thus, for the further analysis it is proposed to use a stationary time section of the installation with a constant shaft rotation frequency. This is a section with an interval of 10 to 20 s.

Accelerometer data has been recorded by an analog-to-digital converter NI USB 6009. The ADC is connected to a computer via a full-speed USB interface and contains eight analog signal input channels (AI), two analog signal generation (AO) channels, 12 digital input / output channels (DIO) and a 32-bit counter.

## III. Algorithm and Methods of Data Extraction and Processing

The bearings have been mounted on the shaft as shown in Figure 2.1. GY-61 ADXL3353 accelerometers have been mounted on the bearing housing. Bearing on position 1 is constant during all experiments. This bearing is new, purchased before starting the experiments. Bearings on position 2 have been previously used in various workbenches and machines and have been replaced from one experiment to another. In this way, the device and feature generation methods aim to classify the bearings on position 2.

The first thirty defective bearings are of type 6204. The rest seventy – 6202. There also has been 7 new bearings of type 6204 and 5 bearings of type 6202. Data collection has been performed using an NI USB-6009 with a sampling rate of 3000 records per second. The speed is determined by an infrared speed sensor. The data was collected according to the acceleration-hold-stop scheme. First, the rotor was accelerated to the desired speed. Then there was a 10-second hold (hereinafter the stationary interval). Then the motor stopped. The recording was carried out for the full load interval.

The resulting dataset consists of 10265700 recordings that describe rotors behavior, 91600 per bearing on average. Collecting data has been uploaded on platform Kaggle and it is in the public domain [13]. The resulting dataset consists of many features, detailed information is presented in table I. For classification, the collected acceleration data of bearings in three axes: X, Y, Z will be used. The name of these features contains the bearing index and the acceleration axis.

TABLE I. Dataset columns description

| **Column name** | ***Description*** | ***Units*** |
|---|---|---|
| Experiment ID | Unique identifier of the experiment; | - |
| Bearing 1/2 ID | Unique identifier of the bearing on the first/second position; | - |
| Timestamp | Time, measured in seconds; | sec |
| A1_X/Y/Z | Acceleration along the X, Y and Z axes for the first bearing; | $m/s^2$ |
| A2_X/Y/Z | Acceleration along the X, Y and Z axes for the second bearing; | $m/s^2$ |
| RPM/HZ | Rotation speed; | rpm |
| W | The motor power at a time. | Watts |

An example of recorded vibration for experiment number 100 is shown in Fig. 3.

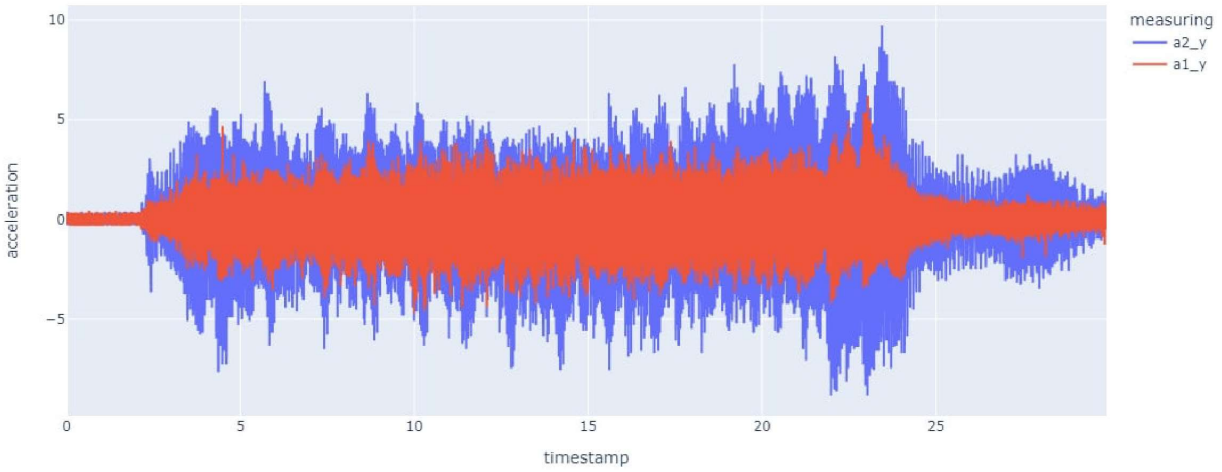


Figure 3. Recorded vibration along the Y axis by two accelerometers

In this paper, it is proposed to use following feature spaces to build classification models:

- Feature space constructed from the values of raw acceleration data on a stationary time interval of the received time series;
- Feature space obtained by evaluating frequency spectrum from the stationary time interval using the fast Fourier transform;
- Space of statistics describing signal behavior;
- Space of statistics describing the frequency spectrum.

The set of statistics have been used in this work is as follows:

*1. Coefficient of variation [14].*

Coefficient of variation (1) is a measure of relative variability.

$$CV = 100\frac{s}{\bar{x}} \tag{1}$$

*2. Range.*

The Range is the difference between the lowest and highest values.

*3. Interquartile range (IQR) [14].*

IQR (2) is the difference between the 25th and 75th percentile of the data. It is a measure of the dispersion similar to standard deviation or variance, but is much more robust against outliers.

$$IQR = Q3 - Q1 \; IQR = \; Q_3 - Q_1 \tag{2}$$

*4. Skewness [14].*

Skewness (3) is the lack of symmetry. The larger values, the greater asymmetry in the distribution of observations.

$$g_1 = \frac{m_3}{m_2^{3/2}}, \tag{3}$$

$$m_i = \frac{1}{N}\sum_{n=1}^{N}(x[n] - \bar{x})^i \tag{4}$$

*5. Kurtosis [14]*

Kurtosis (5) is the extent of the peak in a distribution. The smaller values, the more uniform distribution.

$$g_2 = \frac{m_4}{m_2^2} \tag{5}$$

*6. Entropy [15]*

Entropy is associated with a state of disorder, randomness, or uncertainty. In this paper were used two different ways of measuring Entropy:

*a. Shannon entropy.*

$$H(X) = -\sum_i p_i \; log_2 \; p_i \; , \tag{6}$$

where $N$ is the total number of observed events, and $p_i$ is the probability of the $i$ event.

*b. Sample entropy [16].*

Sample entropy (7) is a modification of approximate entropy, used for assessing the complexity of physiological time-series signals, diagnosis diseased states.

$$SampEn = -log\frac{A}{B}, \tag{7}$$

where A – number of template vector pairs having distance $d[X_{m+1}(i), X_{m+1}(j)] < r$; B – number of template vector pairs having Chebyshev distance $d[X_m(i), X_m(j)] < r$; $r$ – tolerance, $m$ – embedding dimension, $X_m(i) = \{x_i, x_{i+1}, \dots, x_{i+m-1}\}$.

*7. Energy.*

Energy (8) represents time-series signals size.

$$E_x = \int_{-\infty}^{\infty} |x(t)|^2 dt \quad (8)$$

*8. Hjorth parameters [17]*

The Hjorth parameters describe statistical properties in the time domain.

*a. Activity.*

Activity (9) represent signal power, or the variance of time-series.

$$Activity = var(x) \quad (9)$$

*b. Mobility.*

The mobility parameter (10) represents the mean frequency or the proportion of standard deviation of the power spectrum. This is defined as the square root of variance of the first derivative of the signal divided by variance of the signal.

$$Mobility(x) = \sqrt{\frac{var(x')}{var(x)}} \quad (10)$$

*9. Hurst exponent [18].*

Exponent decreases when the delay between two identical pairs of values in the time series increases.

*10. Fractal dimensions [19].*

Fractal dimensions is one of the ways to determine the dimension of a series in a metric space.

*a. Higuchi [19], [20].*

The essence of method is to transform given time-series X(1), X(2), …, X(N) into the new one:

$$X_k^m: X(m), X(m+k), X(m+2k), \dots, X\left(m + \left[\frac{N-m}{k}\right]k\right), \quad (11)$$

where $m = \overline{1,k}$. m and k indicate the initial time and the interval time, respectively. Then Higuchi defines the length of the curve associated to each time series $X_k^m$:

$$L_m(k) = \frac{1}{k}\left(\sum_{i=1}^{\left[\frac{N-m}{k}\right]} \left(X(m+ik) - X(m+(i-1)k)\right)\right)\left(\frac{N-1}{\left[\frac{N-m}{k}\right]k}\right) \quad (12)$$

and takes the average value of the lengths.

*b. Petrosian [19], [21].*

The essence of method is in binarizing given time-series, finding the total number of adjacent symbol changes in the sequence $N_\Delta$ and calculating fractal dimension:

$$F_{Petrosian} = \frac{log_{10}(n)}{log_{10}(n) + log_{10}\left(\frac{n}{n+0.4N_\Delta}\right)} \quad (13)$$

*11. Zero crossing.*

The zero-crossing rate is a statistical feature that describes the number of times that a signal crosses the horizontal axis.

*12. Crest factor.*

The Crest factor (14) defines how extreme the peaks are in a signal.

$$C = \frac{|x_{peak}|}{x_{rms}} = \frac{||x||_\infty}{||x||_2} \quad (14)$$

Fig. 4 shows the Fourier transform for the acceleration signals along one axis of two bearings, one of which is worn out and the other is new. The selected frequencies are from 1 to 400 Hz.

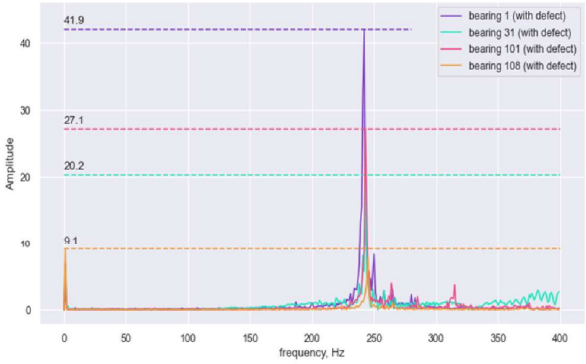


Figure 4. Fourier transform of raw signals

Fig. 5 and Fig. 6 show the cross-correlation of Pearson signals and their spectra respectively along each axis, as well as the rotational speed and power of the engine. The figures show that the correlation between them is rather low. This makes it possible to build linear models based on this data. The figures also show that there is no correlation between the amplitudes and acceleration characteristics of the bench, which complicates the use of empirical approaches to classification.


Figure 5. Pearson correlation for signals

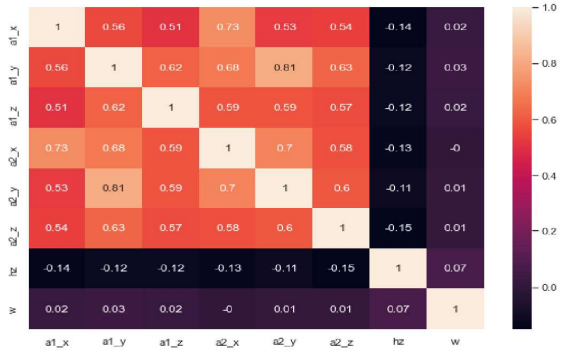


Figure 6. Pearson correlation for signal spectra

Fig. 7 shows the scaled distributions of the selected signal statistics. It could be seen that it is problematic to identify explicit patterns for visual classification based on them.

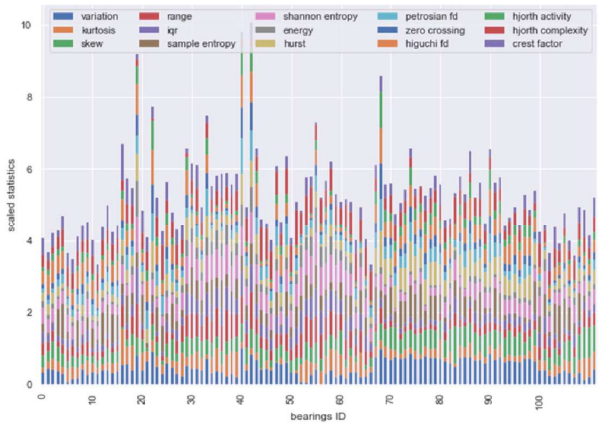


Figure 7. Distribution of signal statistics

Fig. 8 shows a visualization of the distribution of derived quantities from bearing signal statistics. Bearings with and without defects are marked in different colors. Visualization was carried out using the t-SNE method [22]. t-SNE is a tool to visualize high-dimensional data. It converts similarities between data points to joint probabilities and tries to minimize the Kullback-Leibler divergence between the joint probabilities of the low-dimensional embedding and the high-dimensional data. T-SNE has a cost function that is not convex, i.e. with different initializations different results can be obtained. After calculating Pearson's correlation between statistics (Fig. 9), we can come to the conclusion that there is a linear dependence between the presented features. To solve this problem only one statistic from each pair of highly correlated values can be selected.

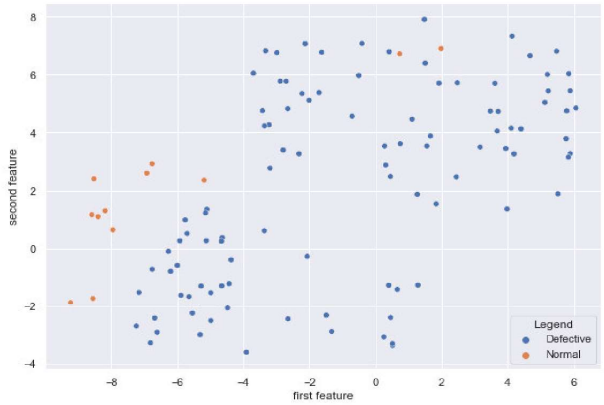


Figure 8. Visualization of derived bearing signal statistics

Fig. 11 shows a visualization of the distribution of the derived quantities from the statistics of the bearing signal spectrum. Features also have been received by t-SNE algorithm. As can be seen from this graph, in contrast to the derivatives of signal features, spectrum features cannot be reduced to a two-dimensional subspace without significant loss of information. Calculation of the correlation (Fig. 12) also showed that there are features with a strong linear relationship. It can also be seen that the correlated features differ from those shown in the signal statistics.

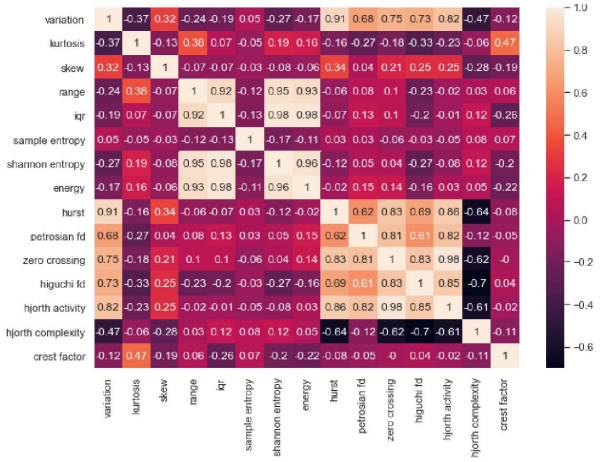


Figure 9. Pearson cross-correlation matrix for one signal

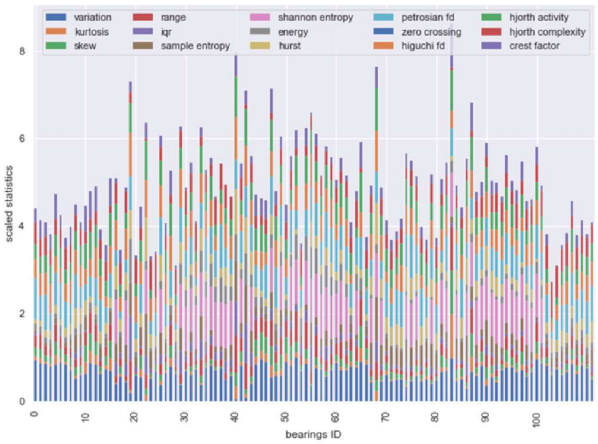


Figure 10. Distribution of signal spectra statistics


Figure 11. Visualization of derived bearing signal spectrum statistics

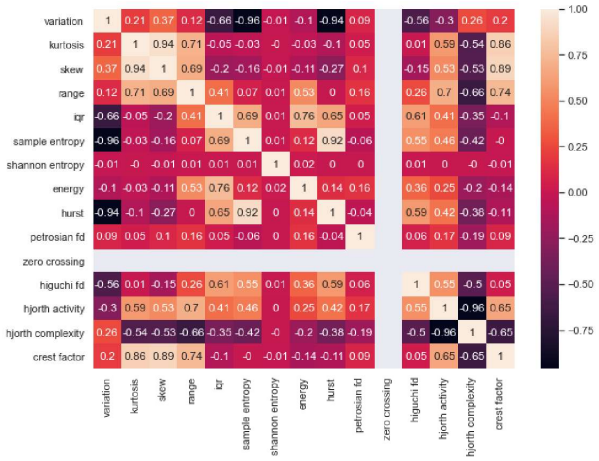


Figure 12. Pearson cross-correlation matrix for spectra of one signal

## IV. Conclusions

The electromechanical part of the experimental bench is a simulator of industrial equipment with rotating units of machines and mechanisms. On-line information about the values of the main vibration parameters flows from the accelerometers to the control unit. The information has been recorded on the computer. Thus, a dataset has been collected for 100 bearings with defects with varying degrees of wear.12 new bearings have been also included in the experiment. In total, two bearing models participated in the experiments: 6204 and 6202. The obtained dataset is proposed to be used to classify bearing defects, to solve the clustering problem by the degree of wear.

The paper proposes four options for processing the received signals to obtain a feature space used in the development of mathematical models for the classification of defected bearings. These approaches are better applicable for different models due to differences in loss of information because of feature space compression, features number and their distribution. Using these approaches, it is possible to build various machine learning models. Thus, the choice of a particular approach depends on the balance between the accuracy and speed of the model.

Thus, the approach used to take signals of vibration sensors and their subsequent processing can be applied in a wide class of problems using various modern methods of data classification. To compare the proposed processing methods, benchmarking is required using various classical machine learning methods, as well as a variety of neural network architectures.

## References


[1] H. Saruhan, S. Sandemir, A. Çiçek, I. Uygur, "Vibration Analysis of Rolling Element Bearings Defects", Düzce University, Facult of Technology, Düzce, Turkey, Journal of Applied Research and Technology, Vol. 12. Issue 3, June 2014, DOI: 10.1016/S1665-6423(14)71620-7

[2] V. E. Yakovlev, P. N. Panochevny "stand diagnostics of vibro bearings by acoustic methods", Pacific National University, "Scientific Notes of PSU" Volume 8, No. 2, 2017

[3] David Kutalek, Milos Hammer, "Vibration diagnostics of rolling bearings using the time series analysis", MM Science Journal, Brno University of Technology, Faculty of Mechanical Engineering, Brno, Czech Republic, 2015, DOI: 10.17973/MMSJ.2015_12_201548

[4] Klychnikov Vladimir Vladimirovich, Lapin Dmitriy Vladimirovich, and Mark Eduardovich Hubbatulin , "Analysis of methods of non-invasive vibroacoustic diagnostics", AIP Conference Proceedings 2318, 090010 (2021). URL: https://doi.org/10.1063/5.0035941

[5] Akimov, Dmitry & Pavelyev, Sergey & Ivchenko, Valery. (2018). "Automated Prediction of Critical States of Turbogenerators During Thermal Expansion of a Rotor and a Stator Based on a Recurrent Neural Network" International Journal of Engineering and Technology(UAE). 7. 37–40. 10.14419/ijet.v7i4.38.24316.

[6] Vladimir Arbuzov, Valery Ivchenko, Ekaterina Matiukhina, Sergey Pavelyev and Andrey Ostroukh "Application of neural network technologies for diagnostics of the technical state of power plant turbo generators based on spectrograms of the vibration measurements", ARPN Journal of Engineering and Applied Sciences, 2018

[7] Davorka Šaravanja, Marko Grbešić, "Application of vibration analysis in journal bearing problems diagnostics", for "30th DAAAM International Symposium on Intelligent Manufacturing and Automation", DOI: 10.2507/30th.daaam.proceedings.013

[8] G. Eason, B. Noble, and I.N. Sneddon, “On certain integrals of Lipschitz-Hankel type involving products of Bessel functions,” Phil. Trans. Roy. Soc. London, vol. A247, pp. 529-551, April 1955. (references)

[9] J. Clerk Maxwell, A Treatise on Electricity and Magnetism, 3rd ed., vol. 2. Oxford: Clarendon, 1892, pp. 68–73.

[10] I. S. Jacobs and C. P. Bean, “Fine particles, thin films and exchange anisotropy,” in Magnetism, vol. III, G.T. Rado and H. Suhl, Eds. New York: Academic, 1963, pp. 271–350.

[11] Y. Yorozu, M. Hirano, K. Oka, and Y. Tagawa, “Electron spectroscopy studies on magneto-optical media and plastic substrate interface,” IEEE Transl. J. Magn. Japan, vol. 2, pp. 740–741, August 1987 [Digests 9th Annual Conf. Magnetics Japan, p. 301, 1982].

[12] M. Young, The Technical Writer’s Handbook. Mill Valley, CA: University Science, 1989.

[13] https://www.kaggle.com/isaienkov/bearing-classification

[14] Zwillinger, D. and Kokoska, S. (2000). CRC Standard Probability and Statistics Tables and Formulae. Chapman & Hall: New York. 2000.

[15] Mera-Gaona, Maritza and López, Diego M. and Vargas-Canas, Rubiel. An Ensemble Feature Selection Aproach to Identify Relevant Features from EEG Signals. Appl. Sci. 2021, 11(15), 6983; doi.org/10.3390/app11156983

[16] Joshua S. Richman, J. Randall Moorman. Physiological time-series analysis using approximate entropy and sample entropy. AJP Heart and Circulatory Physiology, July 2000. DOI: 10.1152/ajpheart.2000.278.6.H2039

[17] Jiang, D.; Ma, Y.; Wang, A.Y. Sleep stage classification using covariance features of multi-channel physiological signals on Riemannian manifolds. Compute. Methods Programs Biomed. 2019, 178, 19–30.

[18] Ding, L.; Luo, Y.; Lin, Y.; Huang, Y. Revisiting the relations between Hurst exponent and fractional differencing parameter for long memory. Phys. A Stat. Mech. Appl. 2021, 566, 125603.

[19] Shi, C.T. Signal pattern recognition based on fractal features and machine learning. Appl. Sci. 2018, 8, 1327.

[20] Chang-Ting Shi. Signal Pattern Recognition Based on Fractal Features and Machine Learning. Appl. Sci. 2018, 8, 1327; doi:10.3390.

[21] Fractal dimension algorithms and their application to time series associated with natural phenomena. F Cervantes-De la Torre et al 2013 J. Phys.: Conf. Ser. 475.

[22] van der Maaten, L.J.P.; Hinton, G.E. Visualizing High-Dimensional Data Using t-SNE. Journal of Machine Learning Research 9:2579-2605, 2008.